# TDR 2006
## Purdue University

### Modeling Structural and Thermal Effects on TDR Measurements in Granular Porous Media

D. A. Robinson, S. B. Jones and S. P. Friedman

Ref.: Robinson, D. A., Jones, S. B. and Friedman, S. P., "Modeling Structural and Thermal Effects on TDR Measurements in Granular Porous Media", Proc. TDR 2006, Purdue University, West Lafayette, USA, Sept. 2006, Paper ID 9, 15 p., https://engineering.purdue.edu/TDR/Papers

# Modeling Structural and Thermal Effects on TDR Measurements in Granular Porous Media

D.A. Robinson [#1,2*], S.B. Jones [#2] and S.P. Friedman [#3]

[1*] Dept of Geophysics, Stanford University, 397 Panama Mall, Stanford, CA 94305; PH (650) 723 3522; email darearthscience@yahoo.com

[2] Dept. Plants, Soils and Biometeorology, Utah State University, Logan, UT 84322.

[3] The Institute of Soil, Water and Environmental Sciences, (ARO) The Volcani Center, Bet Dagan 50250, Israel.

## Abstract

Many empirical formulas, relating TDR-measured permittivity, $K_a$, to volumetric water content ($\theta$) in soils and sediments have been presented, owing to the lack of a robust, and accurate, physically-based model describing this relationship across a range of porous media. Soil-specific calibrations are often infeasible due to the time-consuming gravimetric sampling required for adequate calibration where limited resources often prevail. In this work we continue to develop a physically-based sample scale model for the permittivity-water content relationship in coarse-grained media by including the effect of temperature. In keeping with the development of a physically based grain scale model we incorporate the Kirkwood-Frohlich equation into a layer dielectric model to describe the temperature response of the permittivity of water. The Kirkwood-Frohlich equation contains a parameter '*g*' describing the correlation between water molecules that arises due to hydrogen bonding, and causes cluster formation. These correlated clusters lead to water having a higher permittivity than predicted based on the value of the water dipole moment alone. Though the value of '*g*' can be predicted to within 10% we adopt a pragmatic approach and determine empirical values for '*g*' as a function of temperature to develop an accurate predictive forward model for the thermo-dielectric behavior of granular materials. Our predictions suggest that the greatest temperature affect will be observed in high porosity soils, we therefore test the model against Topp's data for an organic soil and find an encouraging prediction. This work puts the thermo-dielectric response in coarse granular materials on a firm physical footing and suggests a promising modeling avenue for other materials.

**Key Words** Permittivity, dielectric constant, granular media, shape, TDR, calibration.

## Introduction

Topp et al., (1980[1]) proposed a sample-scale empirical calibration between apparent permittivity ($K_a$) measured using time domain reflectometry (TDR) and soil volumetric water content, ($\theta$):

$$\theta = (-530 + 292 \times K_a - 5.5 \times K_a^{\,2} + 0.043 \times K_a^{\,3}) \times 10^{-4} \quad (1)$$

This equation is widely used in coarse and medium-textured soils and has proved very successful. However, the equation takes no account of the permittivity of the components, the porosity, or the geometrical arrangement of the particles. All of these affect the bulk permittivity response that is measured. An alternative approach, providing physical insight into the permittivity response of unsaturated porous media is model development using the 'bottom-up' approach. This approach begins at the grain-scale and endeavors to reconstruct the sample-scale response based on the grain-scale properties. Maxwell (Maxwell, 1881[2]) developed a mixing model approach relevant for describing the electrical conductivity of heterogeneous sands. Since then many dielectric mixing models have been proposed for different applications and geometries (deLoor, 1968[3]; Dobson et al., 1985[4]; Friedman, 1997[5]; Friedman, 1998[6]; Heimovaara et al., 1994[7]; Hilfer, 1991[8]; Hilhorst et al., 2000[9]; Looyenga, 1965[10]). This approach has been used extensively in the geophysics literature where saturated rocks present the simpler case of a two-phase medium (Kenyon, 1984[11]; Sen et al., 1981[12]).

More recently, Robinson et al., (2005[13]) presented a model that treats the porous medium as two dielectric layers composed of 2-phases, air-dry, and water-saturated. The TDR measured apparent permittivity ($K_a$) of a layered material can be derived from the travel time of the TDR signal through layers $L_1$, $L_2$ with combined length of $L = L_1+L_2$:

$$t(L_x) = \frac{L_x}{v_p} \propto L_x \sqrt{K_x} \quad (2)$$

where the subscript x denotes an arbitrary dielectric. Thus, based on square root averaging of the permittivity "refractive index mixture theory", the measured permittivity is:

$$K_a = \left( \frac{L_1 \sqrt{K_1} + L_2 \sqrt{K_2}}{L} \right)^2 \quad (3)$$

This expression has been used previously to model layered soils (Birchak et al., 1974[14]; Topp et al. 1982[15]). Work by, Chan and Knight, (1999[16]), Chan and Knight (2001[17]) and Schaap et al. (2003[18]) showed that this holds for TDR measurements with relatively thick layers such as for wetting fronts in soils and sediments but not for multiple thin layers. Robinson et al.[13] therefore proposed the following equation to describe a bi-layered wetting or drying soil profile:

$$\sqrt{K_a} = \sqrt{\varepsilon_{sat}} \left( \frac{\theta}{\phi} \right) + \sqrt{\varepsilon_{dry}} \left( 1 - \frac{\theta}{\phi} \right) \quad (4)$$

Where, $\theta$ is the mean volumetric water content and $\phi$ is the porosity. The two, two-phase mixture permittivities of saturated ($\varepsilon_{sat}$) and dry materials ($\varepsilon_{dry}$) can be derived from Eq. (4) or measured.

Soils in hot sunny climates exhibit large thermal fluctuations in temperature at the surface, i.e. the upper 0.3m. The thermal gradient can be as much as 30 $^{o}$C over this depth. Attempts to include temperate in calibrations have generally included empirical corrections (Ledieu et al., 1986[19]). These are based on the measured reduction in water permittivity ($\varepsilon_w$) with increasing temperature (T, $^{o}$C) (Weast, 1986[20]):

$$\varepsilon_w(T) = 78.54[1 - 4.579 \times 10^{-3}(T-25) + 1.19 \times 10^{-5}(T-25)^2 - 2.8 \times 10^{-8}(T-25)^3] \quad (5)$$

However, it has been observed that as mineralogy changes to clay minerals the thermo-dielectric response does not agree with empirical prediction (Halbertsma et al., 1995[21]). Or and Wraith (1999[22]) suggested that two competing phenomena occur, a reduction due to increases in temperature and an opposing trend caused by the release of bound water from mineral surfaces. It is therefore important, to develop a physically based description of the thermo-dielectric response that can lay the foundation for further extension of the model; for example to understand the thermo-dielectric behavior of clays. In this work we extend the Robinson et al.[13] approach to account for the effect of temperature on the bulk permittivity response of coarse granular materials.

## Materials and Methods

### Granular Materials and Soils

Two types of media were used to fill TDR cells, 500 μm glass beads (Mo-Sci Corp., Rolla, MO, USA and Trime-IMKO, Germany) and 500 μm quartz grains (Yerucham Crater, Negev desert, Israel). The materials were prepared in the laboratory by washing in de-ionized water and the quartz grains were also acid-washed to remove oxide coatings. The shape of the grains in the quartz sand and sandy soils was assessed using a method described in (Friedman and Robinson, 2002[23]). The method provides an estimate of grain shape based on the slope formed by pouring a granular pile under water. The maximum angle of the poured slope is related to the depolarization factors in the dielectric-mixing model described in the theory section.

The solid phase permittivity of quartz sand and glass spheres was measured using the dielectric immersion method (Robinson and Friedman, 2003[24]; Robinson, 2004[25]). Each material was immersed in 5 dielectric fluids and the point at which the permittivity of the immersion fluid matched the measured effective permittivity gave the permittivity of the solid. The quartz gave a permittivity of 4.7, in close agreement with measurements for crystals (Fontanella et al., 1974[26]), the glass permittivity was determined as 7.6.

## TDR Measurements

Permittivity measurement using TDR is reviewed in Topp and Ferre (2002[27]) and Robinson et al. (2003[28]), in this work, measurements were made using a Tektronix (1502B) TDR cable tester. The TDR was connected to a PC, which was used to collect and analyze waveforms using WINTDR (Or et al., 2004[29]). The TDR was connected to the measurement cell using a 1m RG-58 coaxial cable. The probes were calibrated for effective length using de-ionized water and air. Soil was repacked into the measurement cell and drained while the permittivity was measured with the temperature being kept constant at 25$^{o}$C ±0.5.

## Cell Design, Construction and Packing

The experiments were conducted in custom made, cylindrical (9 cm diameter), 17 cm tall plexiglas containers. At the base of the cylinder groves were machined into the plexiglas, and a porous membrane was fitted over this so that a tension could be applied to drain or wet the cell. The electrodes were mounted in the center of the base of the cylinder, and were made of two parallel, stainless steel plates, 2.5 cm wide, spaced 2 cm apart and 15 cm long. The choice of parallel plates as transmission lines for measurements offer certain advantages for laboratory TDR measurement; a uniformly oriented electrical field is developed and a more even energy distribution (i.e., than rods) is obtained in the sample.

Oven dry materials were packed into the water-filled cells to prevent air entrapment in the sample. The containers were tapped on the bench surface to achieve tight packing. The water content was measured directly knowing the mass of water in the cell. Porosity was independently verified using the particle density and bulk density. Water was drained from the cell through the porous membrane at the base of the cell and subsequently re-wetted through the same membrane. The cell was sequentially drained for water content adjustment over a period of several weeks and then rewetted. Eventually the cell was placed in the oven at 80$^{o}$C and weighed and measured over several weeks to completely dry the material in the cell. It was then re-wetted for the second time, allowing the full range of water content to be measured.

## Theory and Modeling

### Grain-scale Modeling of the Effective Permittivity of a Two-Phase Medium

Perhaps the most widely used two-phase model for describing dielectric spheres in a uniform dielectric background is the Maxwell-Garnett (1904[30]) mixing equation (Sihvola, 1999[31]), given as

$$\varepsilon_{eff} = \varepsilon_0 + 3f\varepsilon_0\left(\frac{\varepsilon_s - \varepsilon_0}{\varepsilon_s + 2\varepsilon_0 - f(\varepsilon_s - \varepsilon_0)}\right) \quad (6)$$

where, $f$, is the volumetric fraction of the solid inclusion (=1-$\phi$, where $\phi$ is the porosity), $\varepsilon_{\text{eff}}$ is the effective permittivity of the two-phase mixture, $\varepsilon_0$ is the permittivity of the

background (water or air) and $\varepsilon_s$ is the permittivity of the granular inclusions. The model assumes that the inclusions and their respective fields are non-interacting, which is an invalid assumption for densely packed granular materials. This interaction effect has been studied theoretically for regular cubic lattices of spheres (Sangani and Acrivos, 1982[32]) and demonstrated experimentally for cubic lattices (Robinson and Friedman, 2005[33]). Recognizing this effect, (Sihvola and Kong, 1988[34]) proposed an, apparent permittivity, $\varepsilon_a$, describing the dielectric constant seen by an individual inclusion (particle or scatterer) in dense packing. Equal to $\varepsilon_0$ in the dilute case, $\varepsilon_a$, in the dense packing is a function of the background and inclusion permittivities and is expected to lie somewhere between the value of the bathing fluid (i.e., water or air) and $\varepsilon_{eff}$:

$$\varepsilon_a = \varepsilon_0 + \alpha(\varepsilon_{eff} - \varepsilon_0) \tag{7}$$

The heuristic parameter, $\alpha$, can be considered physically as representing a polarization resulting from the close packing of the particles. The value of $\alpha$ is confined between 0 and 1. A value of $\alpha = 0$ results in the Maxwell Garnett[30] formula (Eq 2) and $\alpha = 2/3$ and 1 lead to the well known symmetric effective medium approximation (Polder and Santen, 1946[35]) and the coherent potential formulas (Tsang et al., 1985[36]), respectively. A value of $\alpha = 0.2$ was proposed in[23] to properly describe the neighboring particle effects based on measurements in coarse densely-packed random materials. However, it appears that the value changes depending on the ordering of the packing, with $\alpha$ ranging between 0.2 for random packing of monosize spheres and 0.323 for the simple cubic periodic lattice[33].

A further assumption in the Maxwell Garnett model is that of spherical particles, which holds for glass spheres but not for natural granular materials whose shape is expected to cause added polarization. This means that the Maxwell Garnett model is expected to be an upper bound where the background has a higher permittivity than the inclusion (water-saturated media), and a lower bound when this is reversed (air-dry media). The Sihvola and Kong[34] two-phase dielectric mixing model described by

$$\varepsilon_{eff} = \varepsilon_0 + \left\{ \frac{\left[ \sum_{i=a,b,c} \frac{f(\varepsilon_s - \varepsilon_0)\left[\varepsilon_0 + \alpha(\varepsilon_{eff} - \varepsilon_0)\right]}{3\left[\varepsilon_0 + \alpha(\varepsilon_{eff} - \varepsilon_0) + N^i(\varepsilon_s - \varepsilon_0)\right]} \right]}{\left[ 1 - \sum_{i=a,b,c} \frac{fN^i(\varepsilon_s - \varepsilon_0)}{3\left[\varepsilon_0 + \alpha(\varepsilon_{eff} - \varepsilon_0) + N^i(\varepsilon_s - \varepsilon_0)\right]} \right]} \right\} \tag{8}$$

also incorporates particle geometry and provides an implicit equation for calculating the effective permittivity ($\varepsilon_{eff}$) for non zero values of $\alpha$, where the summations are over the three principle axis directions denoted $a$,$b$ and $c$. When $\alpha = 0$ the Maxwell Garnett formula (Eq. 6) results. The effect of particle geometry is modeled using depolarization factors ($N^i$) that describe the extent to which the inclusion polarization is reduced according to its shape and orientation with respect to the applied electrical field. The depolarization factors for an spheroid of revolution (spheroid, $a \neq b = c$) with an aspect ratio

of ($a/b$) can be approximated by the empirical function presented in (Jones and Friedman, 2000[37]):

$$N^a = \frac{1}{1+1.6(a/b)+0.4(a/b)^2} \qquad N^b = N^c = 0.5(1-N^a) \tag{9}$$

The depolarization factors for a sphere/spheroid where *a, b* and *c* are all equal in length are $N^{a,b,c}$ = 1/3, 1/3, 1/3, for thin disks $N^{a,b,c}$ = 1,0,0 and for long needles $N^{a,b,c}$ = 0,0.5,0.5.

The shape factor for the quartz sand was determined from the maximum angle of the slope of the poured granular material, according to the method described in [23]. The measured angle was, 33.0° for the sand; this was converted to the ratio of ($a/b$) for an equivalent oblate particle according to:

$$a/b = 1\text{-}\beta\,(\text{Angle-}23.1)^{0.5} \tag{10}$$

Where $\beta$ is a constant equal to 0.1698 and 23.1 is the maximum slope angle for a pile of spheres. Equation (10) results in an ($a/b$) value of 0.466 for quartz sand.

**Permittivity of water as a function of temperature**

Debye (1929[38]) summarizes his work on dielectrics that led to him receiving the Nobel Prize for his pioneering work on dielectrics; in the book he presents a temperature dependent model describing the permittivity of fluids. The model failed to reproduce the static permittivity of dense fluids and (Onsager, 1936[39]) presented a new model. Neither of these models worked well for fluids with hydrogen bonding. (Kirkwood, 1939[40]) was the first to attempt to account for these forces with a similar model later rederived by Frohlich (1949[41]), the implicit model developed is now termed the Kirkwood-Frohlich (KF) model:

$$\frac{(\varepsilon_w-1)}{(\varepsilon_w+2)}\frac{M}{d}-\frac{(n^2-1)}{(n^2+2)}\frac{M}{d}=\frac{3\varepsilon_w(n^2+2)}{(2\varepsilon_w+n^2)(\varepsilon_w+2)}\frac{4\pi Ng\mu^2}{9kT} \tag{11}$$

Where for the fluid, $\varepsilon_w$ is the permittivity of the fluid, $n$, is the refractive index (1.33 for water), $M$ is the molecular weight (g), $d$, temperature dependent density of the fluid ($gcm^{-3}$), $N$, is Avogadro's number ($6.022\times10^{23}$), $g$, is the correlation parameter (≈2-3), $\mu$, is the gas phase dipole moment ($1.84\times10^{-18}$, Debye), $k$, is the Boltzmann constant ($1.381\times10^{-16}$) and $T$, is the temperature (K). This equation with a value of 1 for '$g$' results in Onsagers equation[39].

**Results and Discussion**

Figure 1 presents data collected from multiple wetting (imbibition) and drying (drainage and evaporation) experiments for the glass spheres and quartz. Plotted on the same graph

are the empirical polynomial equations presented by Topp et al.[1] for Rubicon sandy loam soil, given as:

$$K_a = (2.59 + 21.9 \times \theta + 102 \times \theta^2 - 44.8 \times \theta^3) \quad (12)$$

and 450 μm glass beads, described by:

$$K_a = (3.57 + 31.7 \times \theta + 114 \times \theta^2 - 68.2 \times \theta^3) \quad (13)$$

The figure compares Topp's curves with predictions made using the layer model, (Eq. 4 and 8). This close correspondence with Topp's curve indicates that Eq. (4) is still valid, to some extent, even when the geometry is not that of a sharp wetting or drying front perpendicular to the direction of wave propagation. The general bi-layer refractive index approach adopted in this work should not be confused with the three-phase refractive index model proposed by Whalley (1993[42]). The equation proposed in[42] has proved reasonably successful in an empirical sense. However, strictly speaking it can only be physically applied to a three-layer system, with layering perpendicular to the TDR probe[18].

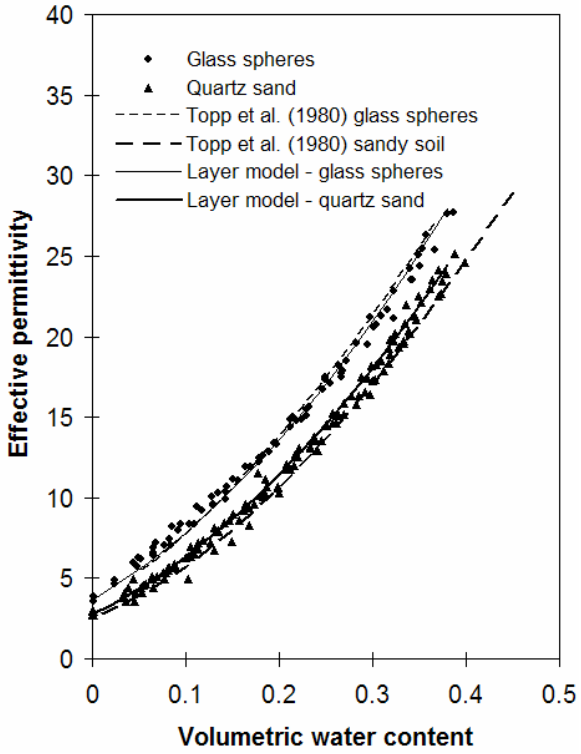


Fig 1. Comparison of permittivity measured using glass spheres and quartz sand with the forward model predictions from the layer model (Eq 4 and 8); also shown for comparison are the empirical calibrations presented by Topp et al.[1] (Eq. 12 and 13).

Temperature is incorporated into the model through the use of the Kirkwood-Frohlich model. The correlation factor '$g$' considers that the preferential parallel alignment of dipole moments results in an enhanced static permittivity ($g$>1). The model has been applied to different polar liquids and values for $g$ determined. Values for $g$ have also been calculated, though these tend to be for single temperatures. Kirkwood[40] suggested originally that $g$ was a function of the coordination number and the bond angle resulting in, $g=1+z\cos^2(\delta/2)$, where $z$ is 4 and $\delta$ is the bond angle (water H-O-H angle ≈ 104.5°). For the case of water this results in a $g$ value of about 2.5. Values have been calculated by various others generally lying between 2 and 3 (Haggis et al., 1952[43]; Lennardjones and Pople, 1951[44]; Oster and Kirkwood, 1943[45]). In this work we determine the value of $g$ from measurements of permittivity as a function of temperature[20] and fit a second order polynomial equation describing $g$ as a function of temperature (°C) for liquid water between 0 and 100 °C, (Figure 2):

$$g = -2E^{-06}T^2 - 0.0028T + 2.8733 \quad (14)$$

Kaatze (2005[46]) suggests that all is not completely clear due to our lack of understanding of the high frequency behaviour of water. A value of 4.3 for the high frequency permittivity of water results in a value of $g$=1 suggesting no correlation. Hasted (1973[47]), also acknowledged this but suggested that measured values of 4.3 still contained dipolar orientation and that it was more appropriate to use the value of the refractive index of water (1.33) in the KF model.

Assuming that it's correct to use the refractive index and that correlation exists, the resulting model fit to the data is compared with the model fit assuming a value of $g$=1 in Figure 3. Hasted suggests that the static permittivity of water will lie between these values, and that the permittivity will be linearly dependent on the number of bonds that the water molecule has. Thus in confined systems or where water interacts with a surface the permittivity of the water could be reduced simply due to a reduction in correlation with other water molecules. It is also conceivable that the opposite could happen. In much of the Earth Science literature it is assumed that the permittivity of water reduces due to physical binding at an interface, however, this analysis suggests that another plausible explanation exists for permittivity reduction in porous media with confining geometries.

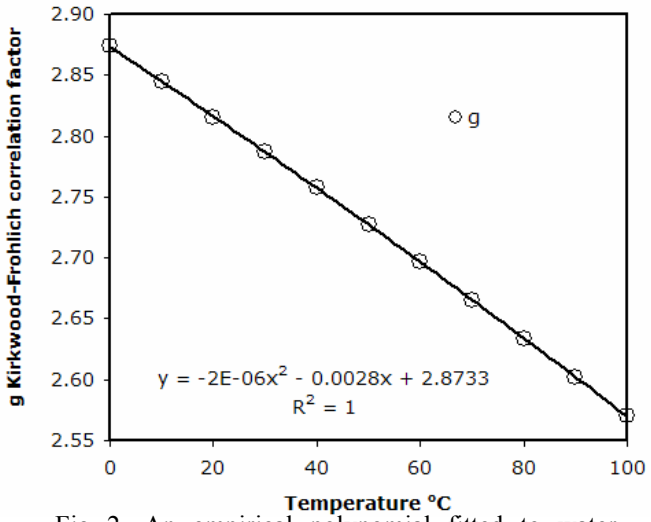


Fig 2. An empirical polynomial fitted to water permittivity data as a function of temperature to determine the value of the correlation parameter '$g$'.

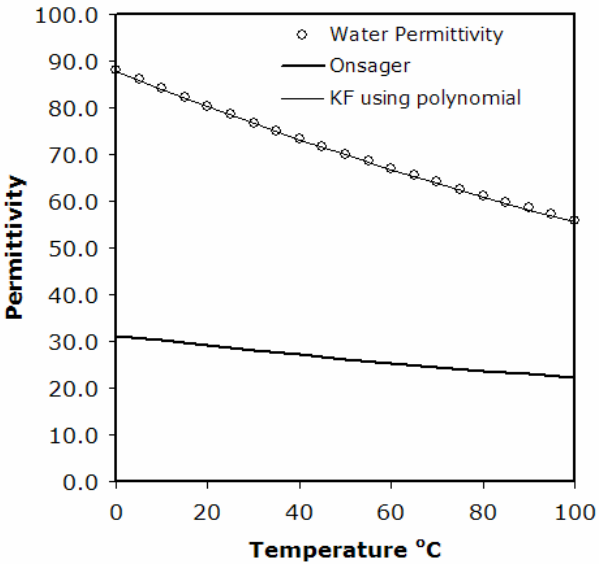


Fig 3. The permittivity of liquid water as a function of temperature with data from [20]. Thick solid line, permittivity of water predicted using the Onsager model (Eq 11 with g=1); Thin solid line, permittivity fitted to data using the Kirkwood-Frohlich[39] model (Eq 11) with '$g$' determined using the polynomial in Fig 2.

Results from forward modelling using Equations (4), (8) and (11) are presented in Figures 4A and 4B. In Figure 4A permittivity as a function of water content for glass spheres

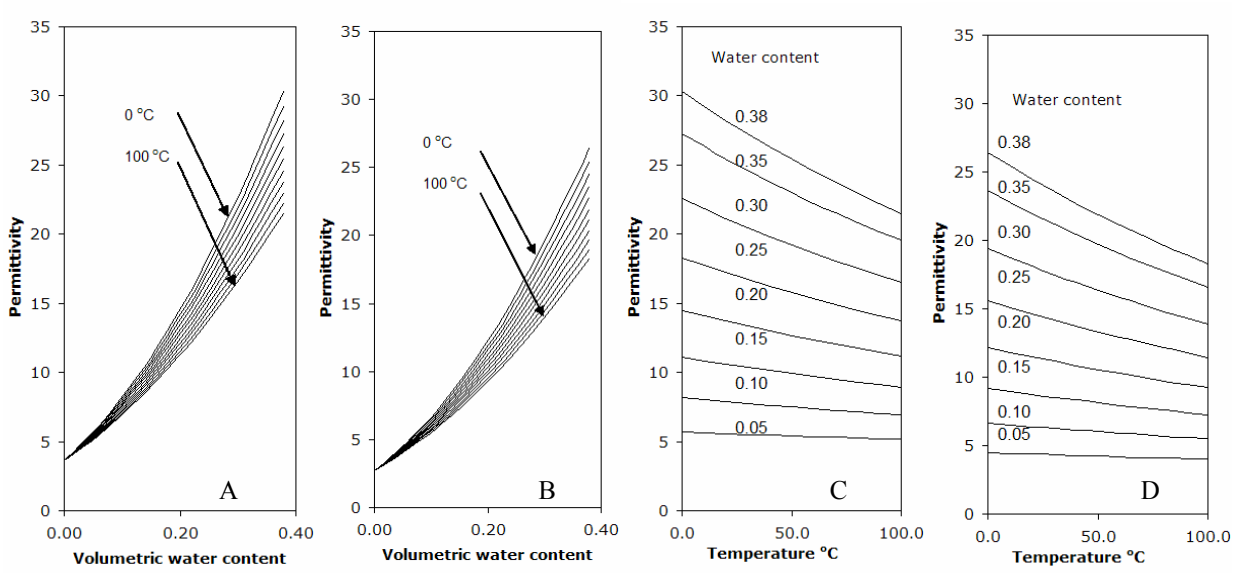


Fig 4 A and B, forward modeling of the expected temperature response of unsaturated glass spheres (A) and quartz sand (B) as a function of water content. C (glass spheres) and D (quartz sand) show the corresponding permittivity change as a function of increasing temperature at fixed volumetric water contents shown.

is presented and in 4B, coarse sand. The figures demonstrate that the temperature effect will be greatest at saturation. Failing to account for temperature changes based on thermal fluctuations of ±10 $^{o}$C from a temperature of 20 $^{o}$C would only result in under- and over-estimation of water content of about 0.01. If the thermal difference is increased to ±20 $^{o}$C from a temperature of 30 $^{o}$C, this results in an under- or over-estimation of about 0.02. This in effect, provides an upper bound on the maximum over- or under-estimation of water content to be expected at these porosities due to thermal fluctuations at the soil surface; where the only significant thermal effect is due to the temperature-dependent permittivity of the water.

As the dielectric contrast between the solid and fluid phases increases so the temperature effect increases. It is therefore to be expected, that the greatest fluctuations will be observed in organic soils that have high porosity, and are composed of organic materials with a permittivity of about 2-3. Topp et al.[1] presented measurements for an organic soil that resulted in the following empirical equation:

$$K_a = (1.74 - 0.34 \times \theta + 135 \times \theta^2 - 55.3 \times \theta^3) \qquad (15)$$

In figure 5 we predict the permittivity of an organic soil, assuming a porosity 0.56 and retaining the shape factor for sand. We compare the results with the calibration equation given in[1] for an organic soil. The first observation is that the layer model gives a surprisingly accurate prediction, indicating in this case that the majority of the divergence from the mineral soil calibration is due to the density/porosity difference, and in this case is not due to bound water, as is so often assumed. Although 'bound' water exists in soils at radio frequencies it has often become common to assume that it's responsible for any deviation below Topp's original empirical curves. This clearly demonstrates that

porosity/bulk density effects account for a large proportion of the observed divergence.

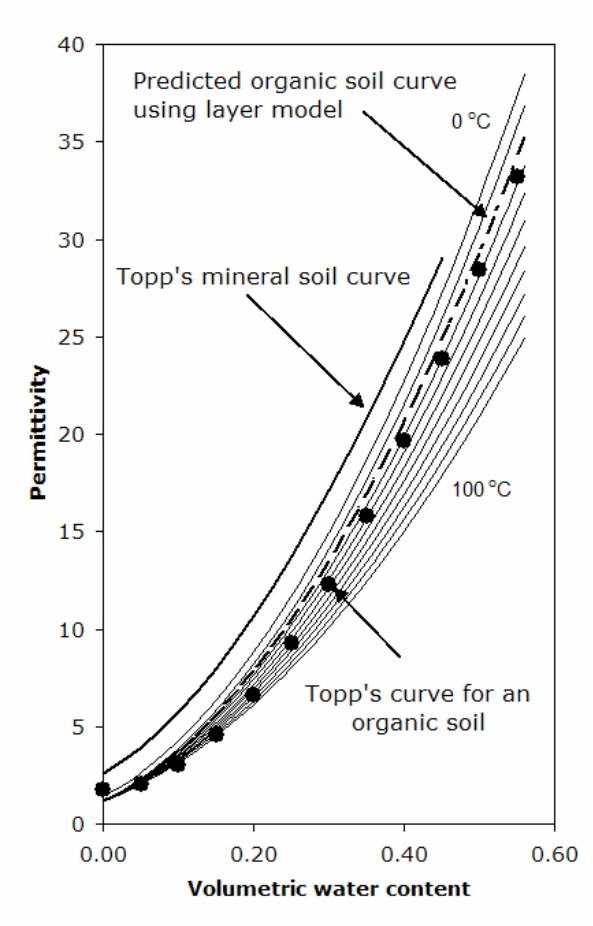


Fig 5 Prediction of the permittivity of the organic soil from Topp et al.[1] with prediction by the layer model. The solid circles are Topp's curve (Eq 15) the dashed line is the prediction from the layer model assuming a permittivity of the solid of 2, which is typical of organic materials. The solid line is Topp's curve for a sandy soil. Close correspondence between forward model and Topp's curve indicate that the divergence from the mineral soil calibration is mostly an issue of porosity, not bound water in this case; peat soils may be expected to contain more bound water and exhibit greater divergence from the prediction.

Repeating the same test for the organic soil, that was conducted for the mineral soil and glass spheres, shows that temperature changes based on thermal fluctuations of ±10 $^{o}$C from a temperature of 20 $^{o}$C, would now result in under and over estimation of water content of about 0.02. If the thermal difference is increased to ±20 $^{o}$C from a temperature of 30 $^{o}$C, this results in an under or ever estimation of about 0.04. In the natural environment this suggests that saturated, organic soils, liable to large daily diurnal fluctuations in temperature, are those most likely to exhibit the greatest error in water content prediction if temperature is not accounted for. In general the results from this work indicate that thermal affects, simply due to changes in the permittivity of water are likely to cause negligible error in water content determination under most circumstances. This work does not account for thermal effects that are present in clays and due to phenomena other than changes in the permittivity of water with temperature.

Finally it is important to point out some of the limitations of the bi-layer modeling approach. First, it addresses only a layered system where one layer is practically water-saturated and the other close to air-dry. The model is designed for a steep wetting/drying front (likely to be encountered in coarse-textured media) and does not describe a distributed water profile. Second, the model does not describe soils with bound water. In order to extend the modeling to a distributed water profile, two additional extension steps are required: (i) the extension of the refractive index averaging towards an effective medium theory, depending upon the steepness of the wetting front

(correlation length of the water content) and the dominant wavelength and (ii) derivation of a proper pore-scale $\varepsilon_{eff}(\theta)$ model following, for example, the approach presented in[6] which would allow different configurations of the air/water phases.

## Conclusions

Results are presented to demonstrate the importance of grain-scale geometry on the sample-scale dielectric response of porous media. The modeling gives insight into the importance of accounting for depolarization caused by close particle packing and particle shape in a two-phase dielectric mixture. Forward model predictions using a layer model are found to correspond exceptionally well with data. Interestingly the model was used to predict the permittivity of an organic soil and demonstrates in this case that divergence from the Topp mineral soil curve is primarily a function of porosity change, negating the need to resort to 'bound' water as an explanation so often relied upon.

The effect of temperature on liquid water from 0-100 $^{o}$C is incorporated into the model using the Kirkwood-Frohlich equation. Predictions indicate that at saturation ($\phi$=0.4) diurnal fluctuations of temperature of sandy soils of ±10 $^{o}$C from a temperature of 20 $^{o}$C, would now result in under and over estimation of water content of about 0.01; and 0.02 if the thermal difference is increased to ±20 $^{o}$C from a temperature of 30 $^{o}$C. Predictions indicate that the greatest error will be observed in organic soils with higher porosity where at saturation ($\phi$=0.56) fluctuations of ±10 $^{o}$C from a temperature of 20 $^{o}$C, would result in under and over estimation in water content of about 0.02, and 0.04 if the thermal difference is increased to ±20 $^{o}$C from a temperature of 30 $^{o}$C. This indicates that under most circumstances in coarse grained soils the effects of temperature on calibration can be expected to be negligible due to the thermo-dielectric response of water. However, in hot dry climates where accurate measurements of small changes in water content are required, temperature can easily be incorporated into a calibration equation. The effect of other temperature dependent phenomena remains to be investigated.

## Acknowledgments

This research was supported in part by research grant No. IS-2839-97, from BARD. The United States - Israel Binational Agricultural Research and Development Fund, and in part by the NSF, grant (04-47287) supporting research to improve instrumentation in the hydrologic sciences through the CUAHSI HMF.

## References


[1] Topp, G.C., Davis J.L., and Annan A.P. (1980). Electromagnetic determination of soil water content: Measurements in coaxial transmission lines. *Water Resour. Res.* 16:574-582.

[2] Maxwell, J.C. (1881). *Treatise on electricity and magnetism.* 2nd ed. Clarendon, Oxford England.

[3] deLoor, G.P. (1968). Dielectric properties of heterogeneous mixtures containing water. *J. Microwave Power* 3:67-73.

[4] Dobson, M.C., Ulaby F.T., Hallikainen M.T., and El-Rayes M.A. (1985). Microwave dielectric behavior of wet soil-Part II: Dielectric mixing models. *IEEE Trans. Geosci. Remote Sensing* GE-23:35-46.

[5] Friedman, S.P. (1997). Statistical mixing model for the apparent dielectric constant of unsaturated porous media. *Soil Sci. Soc. Am. J.* 61:742-745.

[6] Friedman, S.P. (1998). A saturation degree-dependent composite spheres model for describing the effective dielectric constant of unsaturated porous media. *Water Resour. Res.* 34:2949-2961.

[7] Heimovaara, T.J., Bouten W., and Verstraten J.M. (1994). Frequency domain analysis of time domain reflectometry waveforms: 2. A four-component complex dielectric mixing model for soil. *Water Resour. Res.* 30:201-209.

[8] Hilfer, R. (1991). Geometric and dielectric characterization of porous media. *Physical Review* B 44: 60-75.

[9] Hilhorst, M.A., Dirksen C., Kampers F.W.H., and Feddes R.A. (2000). New dielectric mixture equation for porous materials based on depolarization factors. *Soil Sci. Soc. Am. J.* 64:1581-1587.

[10] Looyenga, H. (1965). Dielectric constants of heterogeneous mixtures. *Physica* 31: 401-406

[11] Kenyon, W.E. (1984). Texture effects on megahertz dielectric properties of calcite rock samples. *J. Appl. Phys.* 55: 3153-3159

[12] Sen, P.N., Scala C., and Cohen M.H. (1981). A self-similar model for sedimentary rocks with application to the dielectric constant of fused glass beads. *Geophysics* 46: 781-795

[13] Robinson, D.A., Jones S.B., Blonquist J.M., and Friedman S.P. (2005). A physically derived water content/permittivity calibration model for coarse-textured, layered soils. *Soil Sci. Soc. Am. J.* 69:1372-1378.

[14] Birchack J.R., Gardner C.Z.G., Hipp J.E., and Victor J.M. (1974). High dielectric constant microwave probes for sensing soil moisture. *Proc. IEEE,* vol. 62 1: 93-98.

[15] Topp, G.C., Davis J.L., and Annan A.P. (1982). Electromagnetic determination of soil water content using TDR: I. Applications to wetting fronts and steep gradients. *Soil Sci. Soc. Am. J.* 46:672-678.

[16] Chan, C.Y., and Knight R.J. (1999). Determining water content and saturation from dielectric measurements in layered materials. *Water Resour. Res*. 35:85-93.

[17] Chan, C.Y., and Knight R.J.. (2001). Laboratory measurements of electromagnetic wave velocity in layered sands. *Water Resour. Res*. 37:1099-1105.

[18] Schaap, M.G., Robinson D.A., Friedman S.P., and Lazar A. (2003). Measurement and modeling of the TDR signal propagation through layered dielectric media. *Soil Sci. Soc. Am. J.* 67:1113-1121.

[19] Ledieu, J., Deridder P., Declerck P., and Dautrebande S. (1986). A Method of Measuring Soil-Moisture by Time-Domain Reflectometry. *Journal of Hydrology* 88:319-328.

[20] Weast, R.C. (1986). *Handbook of Chemistry and Physics* CRC Press, Boca Raton, FL.

[21] Halbertsma, J., van den Elsen E., Bohl H., and Skierucha W. (1995). Temperature effects on TDR determined soil water content, In *Proceedings of the symposium: Time-Domain Reflectometry Applications in Soil Science,* S.P. Report No 11, Danish Institute of Plant and Soil Science, Foulum, DK.

[22] Or, D., and Wraith J. M. (1999), Temperature effects on soil bulk dielectric permittivity measured by time domain reflectometry: A physical model, *Water Resour. Res.*, *35*, 371-383.

[23] Friedman, S.P., and Robinson D.A. (2002). Particle shape characterization using angle of repose measurements for predicting the effective permittivity and electrical conductivity of saturated granular media. *Water Resources Research* 38: (11):0043-1397/02/2001WR000746

[24] Robinson, D.A., and Friedman S.P. (2003). A method for measuring the solid particle permittivity or electrical conductivity of rocks, sediments, and granular materials. *Journal of Geophysical Research-Solid Earth* 108: B2 5:1-9

[25] Robinson, D.A. (2004). Calculation of the dielectric properties of temperate and tropical soil minerals from ion polarizabilities using the Clausius-Mosotti equation. *Soil Sci. Soc. Am. J.* 68:1780-1785.

[26] Fontanel.J, Andeen C., and Schuele D. (1974). Low-Frequency Dielectric-Constants of Alpha-Quartz, Sapphire, Mgf2, and Mgo. *Journal of Applied Physics* 45:2852-2854.

[27] Topp, G.C., and Ferre T.P.A. (2002). Water Content, p. 417-545, In J.H. Dane, and G.C. Topp. ed. *Methods of Soil Analysis Part 4 Physical Methods.* Soil Sci. Soc. Am. Inc., Madison, WI, USA.

[28] Robinson, D.A., Jones S.B, Wraith J.M., Or D., and Friedman S.P. (2003). A review of advances in dielectric and electrical conductivity measurement in soils using time domain reflectometry. *Vadose Zone J.* 2:444-475.

[29] Or, D., Jones S. B., VanShaar J. R., and Wraith J. M. (2003), *WinTDR 6.0 Users Guide* (Windows-based TDR program for soil water content and electrical conductivity measurement). Utah Agric. Exp. Stn. Res., Logan, UT, USA.

[30] Maxwell-Garnett, J.C. (1904). Colours in metal glasses and in metallic films. *Trans. Royal Soc.* (London) A 203:385-420.

[31] Sihvola, A. (1999). *Electromagnetic mixing formulas and applications.* Michael Faraday House, Stevenage, Herts, SG1 2AY, UK.

[32] Sangani, A.S., and Acrivos A. (1982). The effective conductivity of a periodic array of spheres. *Proc. R. Soc. Lond. A* 386:263-275.

[33] Robinson, D.A., and Friedman S.P. (2005). Electrical conductivity and dielectric permittivity of sphere packings: Measurements and modelling of cubic lattices,

randomly packed monosize spheres and multi-size mixtures. *Physica a-Statistical Mechanics and Its Applications* 358:447-465.

[34] Sihvola, A.H., and Kong J.A. (1988). Effective permittivity of dielectric mixtures. *IEEE Trans. Geosci. Remote Sens*. 26:420-429.

[35] Polder D. and van Santen J.H.V. (1946). The effective permeability of mixtures of solids. *Physica* 12(5) 257-271.

[36] Tsang, L., Kong L.A., and Shin R.T. (1985). *Theory of microwave remote sensing* Wiley, New York.

[37] Jones, S.B., and Friedman S.P. (2000). Particle shape effects on the effective permittivity of anisotropic or isotropic media consisting of aligned or randomly oriented ellipsoidal particles. *Water Resour. Res.* 36:2821-2833.

[38] Debye, P. (1929). *Polar Molecules* Dover, Mineola, New York.

[39] Onsager, L. (1936). Electric moments of molecules in liquids. *Journal of the American Chemical Society* 58:1486-1493.

[40] Kirkwood, J.G. (1939). The dielectric polarization of polar liquids. *Journal of Chemical Physics* 7:911-919.

[41] Frohlich, H. (1949). *Theory of Dielectrics*. Clarendon Press, Oxford, UK.

[42] Whalley, W.R. (1993). Considerations on the use of time-domain reflectometry (TDR) for measuring soil water content. *Soil Sci*. 44:1-9.

[43] Haggis, G.H., Hasted J.B., and Buchanan T.J. (1952). The Dielectric Properties of Water in Solutions. *Journal of Chemical Physics* 20:1452-1465.

[44] Lennardjones, J., and Pople J.A. (1951). Molecular Association in Liquids .1. Molecular Association Due to Lone-Pair Electrons. *Proceedings of the Royal Society of London Series a-Mathematical and Physical Sciences* 205:155-162.

[45] Oster, G., and Kirkwood J.G. (1943). The influence of hindered molecular rotation on the dielectric constants of water, alcohols, and other polar liquids. *Journal of Chemical Physics* 11:0175-0178.

[46] Kaatze, U., (2005). Electromagnetic wave interactions with water and aqueous solutions. In *Electromagnetic Aquametry* (Ed. Klaus Kupfer), Springer, New York.

[47] Hasted J.B., (1973). *Aqueous Dielectrics*. Chapman and Hall Ltd., London.

**Biographical Information**

David A. Robinson obtained a B.Sc. degree from Reading University U.K. in Soil Science with Sedimentary Geology and a Ph.D. in Soil Hydrology conducted at the Institute of Hydrology and University of Ulster U.K. He is currently a program officer at Stanford University, working with the Consortium of Universities for the Advancement of Hydrologic Sciences Inc. (CUAHSI) as the Operations Director of the Hydrologic Measurement Facility (HMF), Stanford, California.

Scott B. Jones obtained a B.Sc. degree from Brigham Young University in Civil Engineering and from Utah State University he received an M.S. in Agricultural and Irrigation Engineering and a Ph.D. in Soil Physics. He is currently an assistant professor of soil physics at Utah State University in Logan, Utah.

Shmulik P. Friedman obtained a B.Sc. degree and a Ph.D. in Agriculture from the Hebrew University of Jerusalem. He is a research scientist and currently the head of the department of environmental physics and irrigation in the Institute of Soil, Water and Environmental Sciences of the Agricultural Research Organization, Bet Dagan, Israel.